Advanced Steel Construction – Vol. 20 No. 1 (2024) 1–11
DOI:10.18057/IJASC.2024.20.1.1

INVESTIGATION ON BEHAVIOR OF STEEL CABLES SUBJECT TO LOCALIZED FIRE IN LARGE-SPACE BUILDINGS

Xiu-Shu Qu [1], Yu-Xiang Deng [1] and Guo-Jun Sun [2, *]

[1] *School of Civil and Transportation Engineering, Beijing University of Civil Engineering and Architecture, Beijing,100044,China*
[2] *Faculty of Architecture, Civil And Transportation Engineering, Beijing University of Technology, Beijing 100124, PR China*
* *(Corresponding author: E-mail: sunny2369@163.com)*

ABSTRACT

Pre-tensioned steel cable is a crucial load-bearing component of steel structure, the fire behavior of which affects the overall performance of the structure. However, it presently lacks research and fire safety design method to consider steel cable members subject to localized large-space building fire. In this paper, the mechanical behavior of normal steel strand cable and full-locked steel cable under large-space building fire is investigated, to provide guidance for the fire safety design of steel cable. Firstly, the numerical model of temperature field of steel cables subject to large-space building fire was established and verified with the test results. Secondly, based on the verified temperature field model, the sequential thermal-mechanical coupling numerical model was established to study the fire behavior of steel cable, including temperature field, temperature gradient, failure mechanism, internal force and contact stress. Thirdly, the numerical method was adopted for the parametric analysis on the fire resistance of steel cables, considering the effect of temperature-field model, non-uniform fire, load ratio and span of steel cable. The following conclusions are obtained: 1) The average temperature can be taken to simplify the transverse temperature field due to the small amplitude of transverse temperature gradient of steel cable section; 2) Because of the size effect of steel wire, the overall temperature of normal steel strand cable is higher than that of full-locked steel cable under the same conditions of same nominal diameter and fire conditions, and the damage occurs earlier than that of full-locked steel cable under fire.

ARTICLE HISTORY

Received: 8 December 2022
Revised: 8 June 2023
Accepted: 27 August 2023

KEYWORDS

Fire in large-space building;
Steel cable;
Failure mechanism;
Fire resistance

1. Introduction

Spatial cable-truss structure is a widely used large-space steel structure. At present, in addition to focusing the static or dynamic properties of cable-truss structure, people begin to pay attention to the influence of length errors, structural layout optimization, construction forming optimization on the performance of cable-truss structure [1][2][3][4]. With the development of urban construction, the fire accidents occur more and more frequently in buildings. Scholars have started to focus on the phenomenon of a decline in the overall load-bearing capacity of large-space steel structure caused by cable rupture under fire, which can result in the further progressive collapse of whole steel structures. The studies [5][6] show the high-temperature environment caused by fire has a negative effect to reduce the material strength of steel cables, affecting the load distribution of overall structure, the evaluation of the fire-resistant capacity of steel cable members in engineering design practice is important. Thus, it is essential to study the fire behavior of steel cables subject to localized fire in large-space buildings, providing research basis to develop the fire safety protection standards for steel cable.

In the early 1950s, Frank Day et al. [7] conducted a preliminary elevated temperature test on the prestressed steel wires used for concrete components. Gales et al. [8] and Hou et al. [9] studied the mechanical performance of prestressed steel wires with different strength under high temperature. It was found that the additional prestress loss caused by high-temperature creep under fire impacts significantly on the fire-resistant limit of structure. Sun et al. [10] investigated the mechanical behaviors of Z-shape steel wire under elevated temperature, the modified two-stage Ramberg-Osgood model of which was proposed to present the constitutive relationship. With the further researches were conducted, the studies of the fire behaviors of prestress steel cables are focused. Zong et al. [11], Kotsovinos et al. [12], Du et al. [13][14][15] and Sun et al. [16][17][18] carried out the steady-state tests of the steel cables with different strength, including normal steel strand cable, stainless steel cable, parallel wire cable, etc., concentrating on the fire behaviors of material including the stress-strain relationship at elevated temperature, the reduction laws of mechanical properties and the high-temperature creep. Du et al. [19] conducted the post-fire tensile tests on Grade 1670 steel wire, the fitting equations of post-fire mechanism performance for the steel wire were proposed. Sun et al. [20], Fontanari et al. [21][22] conducted transient thermal simulations on normal steel strand cables, steel wire ropes and parallel wire cables subject to ISO-834 fire, the mechanical behavior and the temperature field of which under continuous temperature history were studied comprehensively.

At present, the studies of the fire behaviors of steel cables mostly concentrate on the steady-state heating study or the transient thermal study based on the ISO-834 fire. However, the investigations on the fire behaviors of steel cables subject to large-space building fire in transient heating condition are not fully carried out. In this paper, the numerical method is used to analyze the temperature field and the tensile fracture mechanism of steel cables under the large-space building fire, to reveal the thermo-mechanical behaviors of normal steel strand and full-locked steel strand, including failure mode and redistribution of internal force in fire. Furthermore, the parametric study on the fire resistance is performed to clarify the main factors that affect the fire-resistant capacity of steel cables in the large-span fire condition.

2. Setup and validation of numerical models

2.1. Development of thermal FE model

2.1.1. Temperature-field model for fire in large-space building

The ISO-834 curve recommended by the specification "Code for fire safety of steel building structures" (GB 51249-2017) [23] is mainly appropriate to indoor fire scene of small space, but not applicable to the fire scene in which the steel cable components subject to the large-space building fire. The literature [24] was referred in this paper, and the temperature-time curve applied to the fire behavior investigation on steel cable was introduced to depict the large-space fire:

$$\mathrm{T(x,H,t)} = \mathrm{T_g(0)} + \mathrm{T_g^{max}}(1 - 0.8\mathrm{e^{-\gamma t}} - 0.2\mathrm{e^{-0.1\gamma t}}) \cdot \mathrm{K_{sm}} \tag{1}$$

$$T_g^{max} = (20Q + 80) - (0.4Q + 3)H + (52Q + 598) \times 10^2/A_{sp} \tag{2}$$

$$K_{sm} = \beta + (1 - \beta)e^{(D/2-x)/7} \tag{3}$$

$$D = 2\sqrt{A_q/\pi} \tag{4}$$

Where $T(x,H,t)$ is the air temperature (℃) when the calculation location is x (m) from the fire source center and H (m) from the ground; T_g^{max} is the maximum air temperature; Q (MW)is the heat release rate; A_{sp} (m^2) is the floor area; A_q (m^2) is the fire area; γ is the factor of fire growth type; K_{sm} is the factor for regression ratio of maximum air temperature; β is the shape factor related to space height and the floor area.

2.1.2. Thermal FE model setting

The FE software Abaqus is used to analyze the thermal behavior of steel cable under the large-space fire. The unit DC3D8 was applied as the heat transfer element for the model. The thermal boundary conditions of thermal radiation and convective heat transfer were respectively set on the surface element of steel cables, and a closed-cavity radiation condition was established on the surface

element of inner steel wires. In reference to European specification [25], the convective heat transfer coefficient was taken as $25W{\cdot}m^{-2}{\cdot}K^{-1}$, the Stefan-Boltzmann constant was set as $5.67\times10^{-8}w/(m^2\cdot K^4)$, the surface heat emission was set as 0.8. In reference to the European specification [26], the cavity heat emission was taken as 0.8; the initial ambient temperature was 20℃. In the process of thermal simulation, the thermal contact resistance between steel wires was ignored, and the interaction between the steel wires was simulated by the "tie-boned" contact.

2.1.3. Thermal parameters of materials

The density of steel was taken as $7850\,kg\cdot m^{-3}$. In reference to the European specification [27], the thermal conductivity of steel λ_s ($W\cdot(m^2\cdot℃)^{-1}$) was taken as $\lambda_s=52.57-1.541\times10^{-2}T_S-2.155\times10^{-5}{T_S}^2$, and the specific heat capacity c_s ($J\cdot(kg\cdot℃)^{-1}$) was taken as $c_s=470+20\times10^{-2}T_S+38\times10^{-5}{T_S}^2$, where T_{st} (℃) is the temperature of steel material.

In reference to the specification [23], when verifying the thermal FE model, the equivalent thermal conductivity of non-swelling fire protection coating λ_i ($W\cdot(m^2\cdot℃)^{-1}$) and the equivalent thermal resistance of intumescent fire protection coating R_i ($(m^2\cdot℃)\cdot W^{-1}$) were taken as follows:

$$\lambda_i=\frac{d_i}{\frac{5\times10^{-5}}{(\frac{T_S-T_{S0}}{t_0}+0.2)^2-0.044}\times\frac{F_i}{V}} \tag{5}$$

$$R_i=\frac{5\times10^{-5}}{\left(\frac{T_S-T_{S0}}{t_0}+0.2\right)^2}\times\frac{F_i}{V} \tag{6}$$

Where $\frac{F_i}{V}$ is shape factor of cross-section of steel cable with fire protection coating; T_{s0} (℃) is initial temperature of steel cable before heating; T_s (℃) is average temperature of steel cable; t_0 (s) is the time of the temperature of steel cable reaching average temperature.

2.2. Development of mechanical finite element

2.2.1. Mechanical FE model setting

In the finite element analysis, the unit C3D8R was adopted as the element of mechanical analysis. In terms of mechanism, the interaction between steel wires was simulated by the general contact, in which the tangential friction coefficient was taken as 0.3 and 'hard contact' was applied for the normal contact simulation. In the setting of the boundary conditions at both ends of the steel cable, it was assumed that the steel cable was completely constrained to the anchoring devices. Thus, the displacement boundary condition of the unloaded end of the steel cable was set to be completely fixed, and that of the loaded end was only released the displacement degree of freedom that was consistent with the loading direction.

2.2.2. Mechanical parameters of material

It is essential to fully take account of deterioration of material, thermal creep and thermal expansion when the steel cable is under the fire conditions. In referrence to the test results of the literature [15], the stress-strain relationship for steel at elevated temperature is adopted as follows:

$$\sigma=\begin{cases}E\varepsilon & ,0\leqslant\varepsilon\leqslant\varepsilon_{\mathrm{pp},\theta}\\ f_{\mathrm{pu},\theta}-\left(a_1e^{-(\varepsilon/a_2)}+a_3\right) & ,\varepsilon_{\mathrm{pp},\theta}<\varepsilon\leqslant\varepsilon_{\mathrm{pt},\theta}\\ b_1\varepsilon^2+b_2\varepsilon+b_3 & ,\varepsilon_{\mathrm{pt},\theta}<\varepsilon<\varepsilon_{\mathrm{pu},\theta}\\ 0 & ,\varepsilon\geqslant\varepsilon_{\mathrm{pu},\theta}\end{cases} \tag{7}$$

Where the coefficients a_1,a_2,a_3,b_1,b_2,b_3 are the factors fitting the regression formula, the specific values refer to the literature [15]; σ (MPa) is the stress of steel wires; ε is the strain of steel wires; E (MPa) is the elastic modulus of steel wires at elevated temperature; $\varepsilon_{\mathrm{pu},\theta}$ is the rupture strain at elevated temperature; $\varepsilon_{\mathrm{pp},\theta}$ is the proportional limit strain at elevated temperature; $\varepsilon_{\mathrm{pt},\theta}$ is the limit strain for yield strength at elevated temperature.

In reference of the literature [28], the thermal expansion coefficient is acquired as follows:

$$\varepsilon_{\mathrm{th}}=1.87\times10^{-9}\times T^2+1.22\times10^{-5}\times T-3.14\times10^{-4} \tag{8}$$

$$\alpha_{\mathrm{T}}=\frac{\mathrm{d}\varepsilon_{\mathrm{th}}}{\mathrm{d}T}=3.74\times10^{-9}\times T+1.22\times10^{-5} \tag{9}$$

Where $\varepsilon_{\mathrm{th}}$ is the strain caused by thermal expansion; α_{T} is the thermal expansion coefficient; T (℃) is the temperature of steel wires, ranging from 20℃~800℃.

The thermal creep coefficient of steel cables at elevated temperature is calculated as follows:

$$\varepsilon_{\mathrm{cr}}=\frac{c_1}{c_3+1}\sigma^{c_2}t^{c_3+1}\mathrm{e}^{-\frac{c_4}{T}}+c_5\sigma^{c_6}\mathrm{e}^{-\frac{c_7}{T}} \tag{10}$$

Where $\varepsilon_{\mathrm{cr}}$ is the creep strain at elevated temperature; c_1~c_7 are the regression parameters in reference of the literature [28]; t (min) is the heat up time.

2.3. Validation of FE model

To verify the FE model in analysis of the fire behavior of steel cables, the thermal FE model was established, and its simulated results were compared with the test result of the specimens with fire protection reported by the literature [29]. In the thermal FE model, the mesh division of the specimen with the non-swelling fire protection coating and the specimen with the intumescent fire protection coating is presented in Fig.1. Fig.21 shows the comparative results of the simulation and the test, where Δ (mm) denotes the distance from the checkpoint to the surface of the steel cable, d (mm) denotes the thickness of the fire protection, D (mm) denotes the diameter of the steel cable.

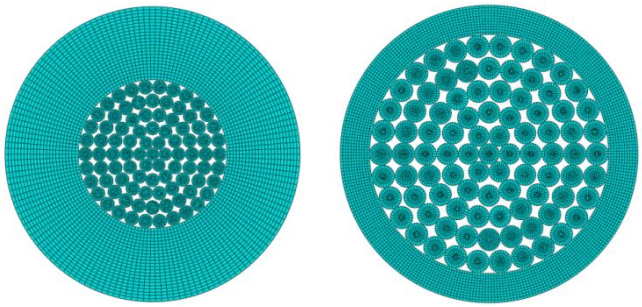

(a) Non-swelling fire protection coating (b) Intumescent fire protection coating

Fig. 1 Mesh division of specimens

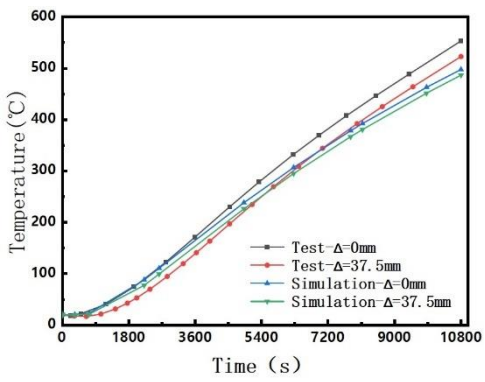

(a) d=50mm, D=75mm

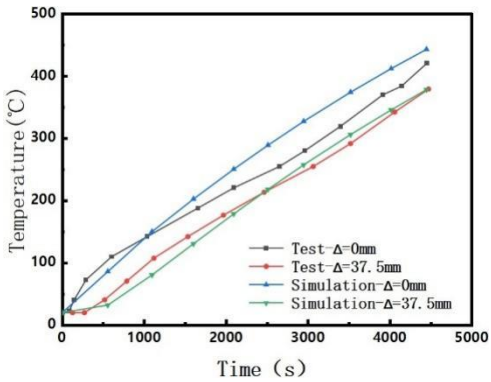

(b) d=10mm,D=75mm

Fig. 2 Time-temperature curve of specimens

The simulation result of the specimen with the non-swelling fire protection coating shown in Fig.2 (a) was nearly consistent with the experimental result, while the simulation result of the specimen with the intumescent fire protection coating shown in Fig.2 (b) had a certain error. The reason for the difference in the fitting degree of the two species is that, the actual thermal conductivity of non-swelling fire protection coating is relatively stable in heat up time, changing little over the elevated temperature. Therefore, the temperature field of the specimen with the non-swelling fire protection coating can be well simulated by adopting the equivalent thermal conductivity of the non-swelling fire protection coating in reference to the specification [23]. However, the thickness of the intumescent fire protection coating changes dramatically during the thermal expansion phase, and the actual thermal conductivity of which varies greatly over the elevated temperature [30]. Thus, the simulation deviation exists in the temperature of the specimen surface, approaching to 5%~10% during the thermal expansion phase, when the actual thermal resistance of the intumescent fire protection coating is replaced by the equivalent thermal resistance in reference to the specification [23]. Though the deviation existed in the simulation, it was still generally within a reasonable range, the numerical model can still be adopted as the reference for subsequent analysis.

3. Fire behavior of steel cable in large-space fire

3.1. Specimen design

The normal steel strand cable and the full-locked steel cable were chosen as the study specimen in this paper. The diameter of the round steel wire used in the specimens was 7 mm. The height of the Z-shape steel wire was 7 mm and the area was 51.32 mm^2. The diameter of the steel cable was 35 mm. The length was 2500 mm. The second layer of twist angle was 7.2° and the third layer of which was 14.4°. The type of the steel cable was 1×19.

The numerical simulation of monotonic tension at room temperature was carried out on the steel cables. The ultimate break force of the normal steel strand cable was 1264.07 KN, and the ultimate break force of the full-locked steel cable was 1459.96 KN. In the simulation, the load ratio was 0.7.

3.2. Parameters of uniform and non-uniform fire distribution

In this section, the fire scenario is simulated according to the temperature-field model of the large-space building fire stated in Section 1.1. Equation (1) ~ (4) indicates the meaning of physical parameters in the large-space building fire model, including floor area A_{sp}, position height H, heat release rate Q, factor of fire growth type γ, effective diameter of the fire source D and regression ratio of the fire K_{sm}. In this paper. The large-space building refers to the building space with a floor area of no less than 500 m^2 and a space height of no less than 4 m [31]. The setting parameters of the uniform and non-uniform fire distribution within the definition of large-space building were set as follows: The floor area A_{sp} was 500; the position height H was 6 m; the heat release rate Q was 25 MW; the factor of fire growth type γ was 0.004.

For the uniform fire condition, the effective diameter of the fire source was 2500 mm, covering the longitudinal span of the steel cable; for the non-uniform fire condition, the effective diameter of the fire source was 1000 mm, and the non-uniform fire was set below the median part, the regression ratio of the fire K_{sm} was taken as 0.6. The detail arrangement of the fire source under the non-uniform and the uniform fire distribution are presented in Fig.3.

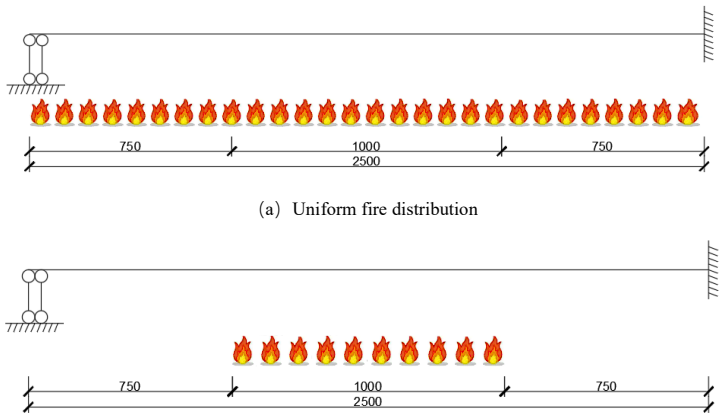

(a) Uniform fire distribution

(b) Non-uniform fire distribution

Fig. 3 Arrangement of fire source

3.3. Judging criteria of fire resistance

In the simulation, the judging criteria of the fire resistance of steel cable was adopted in reference to the literature [15]. The total strain of the mechanical element of the steel cable is composed of mechanical strain, thermal creep strain and thermal expansion under the thermo-mechanical coupling condition. As the total strain reaching the failure criterion of its rupture strain or the element achieving ultimate strength at elevated temperature, it is judged that the steel cable loses the fire-resistant capacity, reaching the fire resistance. The element of the FE model in the analysis should be checked by the following criterion:

$$\sigma_{p,\theta} \le f_{pt,\theta} \tag{10}$$

or

$$\varepsilon_{total} \le \varepsilon_{pu,\theta} \tag{11}$$

Where $\sigma_{p,\theta}$ is the total stress of the element at elevated temperature; $\varepsilon_{pu,\theta}$ is the rupture strain of steel wire at elevated temperature; ε_{total} is the total strain of the element; $f_{pt,\theta}$ is the ultimate strength of steel wire at elevated temperature.

3.4. Analysis of temperature field of steel cable

Under both the non-uniform fire and the uniform fire distribution conditions, the temperature fields of the two types of the steel cables were analyzed for 180 min. In the uniform fire condition, both the center and the surface of the steel cables were taken as the temperature measuring points, the layouts of which are presented in Fig.4 (a)(b). For the non-uniform fire condition, the measuring positions of temperature arranged along the longitudinal span of steel cable are presented in Fig.4 (c), where the center of cross section was taken as the temperature measuring point.

3.4.1. Temperature field

Under the uniform fire condition, the temperature field of the transverse sections and the temperature development of the measuring points are presented in Fig.5 (a)(b); under the non-uniform fire condition, the temperature development of the longitudinal measuring points of the steel cables is presented in Fig.6. It can be seen from Fig.5 and Fig.6, under the two types of the fire conditions, the transverse temperature and the longitudinal temperature of the normal steel strand cable was higher than that of the full-locked steel cable. At the measuring position Z6, the peak temperature for the normal steel strand cable was 588.5°C, and the peak temperature of the full-locked steel cable was 468.14°C; at the measuring position Z1, the peak temperature of the normal steel strand cable was 509.67°C, and that of the full-locked steel cable was 388.37°C. It indicated that the strength deterioration of the normal steel strand cable occurred earlier than that of the full-locked steel cable.

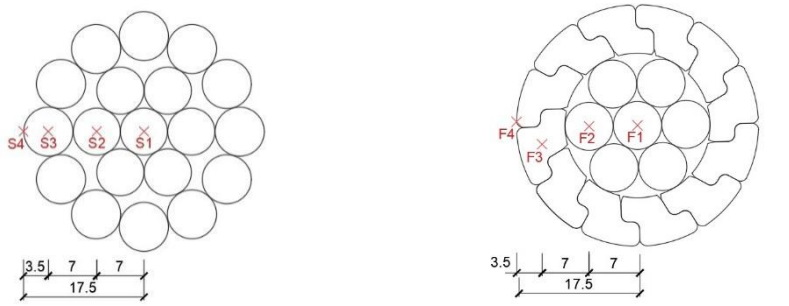

(a) Transverse section of normal steel strand cable (b) Transverse section of full-locked steel cable

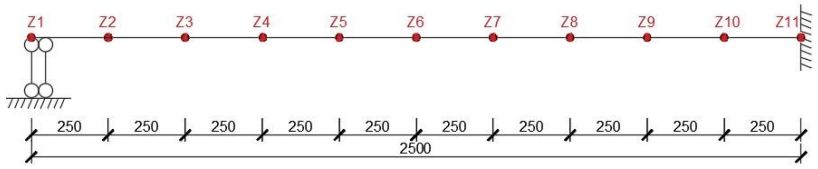

(c) Longitudinal measuring position

Fig. 4 Layout of temperature measuring position

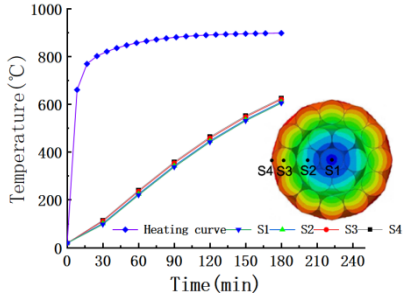

(a) Normal steel strand cable

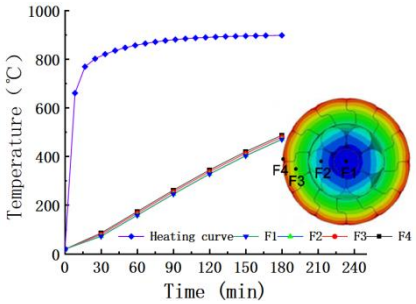

(b) Full-locked steel cable

Fig. 5 Transverse temperature field of steel cable under uniform fire

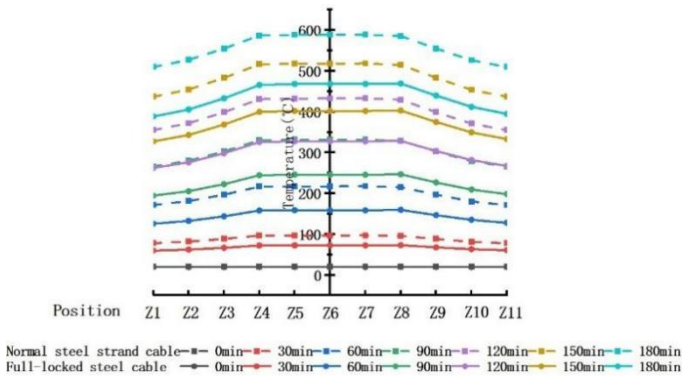

Fig. 6 Longitudinal temperature field of steel cable under non-uniform fire

To reveal the difference of the temperature field between the two types of the steel cables, the temperature measuring points at the same position of the two steel cables were compared. Under the uniform fire, the measuring points S4 and F4, S1 and F1 were taken in comparative analysis, Fig.7 (a) shows the comparative result. Under the non-uniform fire condition, the measuring points Z6 at fire position and the measuring points Z1~Z3 at non-fire position were compared, Fig.7(b) shows the comparative result.

As shown in Fig.7, for the two types of fire conditions, the temperature of the normal steel strand cable was higher than that of the full-locked steel cable, and the temperature difference continued to expand with time. In the condition of uniform fire, the peak temperature difference between the surfaces of the two types of steel cables was 138.30 degrees; under the non-uniform fire, the peak temperature difference between the two was 122.05 °C. Moreover, the temperature difference of the two steel cables decreased with the distance from the measuring point to the fire resource increased. The reason for this phenomenon is that, under the condition of the same section diameter, the geometric curvature of the third layer of steel wires of the normal steel strand cable is higher than that of the full-locked steel cable, there is the size effect leading to more heat absorption during the heating process [20].

At the same time, due to the steel ration of the full-locked steel cable higher than steel ration of the normal steel strand cable, the temperature development of the full-locked steel cable in the longitudinal direction lagged that of the normal steel strand cable.

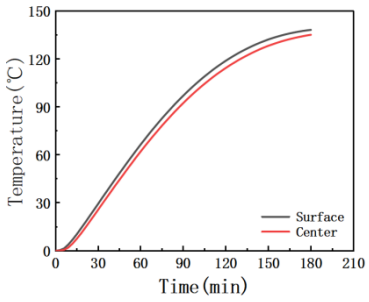

(a) Uniform fire condition

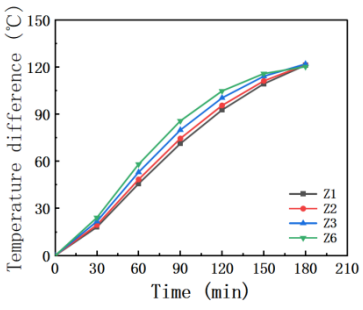

(b) Non-uniform fire condition

Fig. 7 Comparison of temperature field of steel cables

3.4.2. Temperature gradient

The transverse temperature gradient was obtained by calculating the temperature difference between the measuring points S4 and S1, F4 and F1, while the longitudinal temperature gradient was acquired by calculating the temperature difference of the center wires of the two types of the steel cables at the measuring point Z6 and Z1. Fig.8 shows the results of the temperature gradient .

As shown in Fig.8 (a)(b), under both the uniform fire and the non-uniform fire, the peak value of the transverse temperature gradient of the two types of the steel cables was small, the normal steel strand cable was 22℃, and the full-locked steel cable was 17℃. It shows that the extent of the stress redistribution caused by the transverse temperature gradient is low. To simplify the calculation in fire design, it is recommended that the transverse temperature field can be simplified by taking the average temperature of the section. However, as shown in Fig.8 (c), the peak value of the longitudinal temperature gradient was large, the normal steel strand cables was 81℃, and the full-locked steel cable was 79℃, which cannot be ignored in fire design.

There was the large difference between the longitudinal temperature gradient and the transverse temperature gradient. This is mainly because the heating rate of the non-fire part of the steel cable is much smaller than that of the fire part, and there is a lag in the longitudinal transfer of heat flux from the higher temperature area to the lower temperature area along the cable length. In the example, the temperature hysteresis phenomenon of the non-fire part tends to be more obvious with the increase of the distance from the fire part.

It is noted that Fig.8 shows the descending period of the temperature gradient when the steel cables were in the later stage of the heat up time. The reason is the thermal conductivity λ_s decreases and the specific heat capacity c_s increases when the temperature increases, so the rate of temperature increment of the steel cables declines with the heat up time. While during the process of heat transfer from high temperature position to low temperature position, the thermal lag behavior exists between the surface and the center of the transverse section, and also exists between the longitudinal measuring point Z6 and Z1. The temperature-elevation rate of the measuring point with relatively higher temperature first declines compared with the measuring point with lower temperature, and therefore the temperature gradient decreases during the later stage of the heating process.

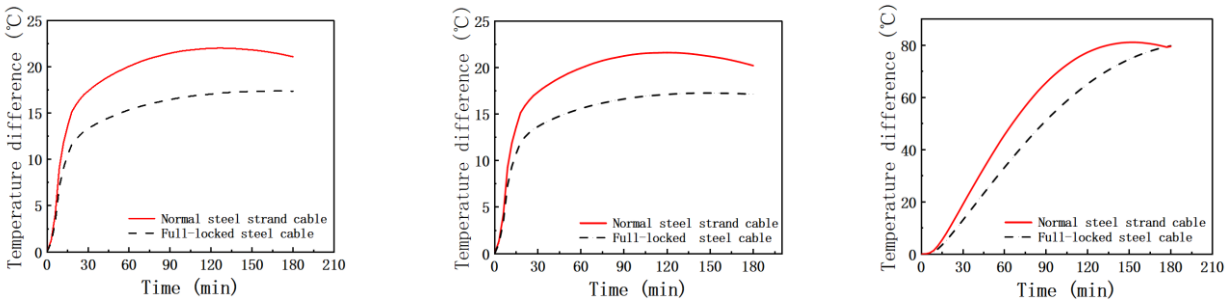

(a) Transverse gradient in uniform fire (b) Transverse gradient in non-uniform (c) Longitudinal gradient in non-uniform

Fig. 8 Temperature gradient of steel cables

3.5. Mechanism analysis of steel cable

3.5.1. Damage development and mode

Fig.9 shows the damage locations and modes of the steel cables under uniform fire and non-uniform fire conditions. It can be found that the steel cables mainly experienced three stages of necking, spiral decoupling and breakage when working in a fire environment.

In the stage of necking, the first layer and the second layer of steel wires entered the yield stage, the deformation development of the steel wires was accelerated. The necking phenomenon was intensified with the elevated temperature.

In the stage of spiral decoupling, all the steel wires entered the plastic stage, and the deformation of the steel wires developed rapidly. The torsional moment produced in the inner part of the steel cables caused the second and the third layer of steel wires to spread out to different extent.

In the stage of breakage, when the steel cable was subject to the uniform fire, the center steel wire firstly ruptured at the position where the necking phenomenon occurred near the end of the steel cable, then was pulled out. When the steel cable was subject to the non-uniform fire, the center steel wire firstly ruptured near the boundary of the fire position and the non-fire position. The second and the third layer of steel wires were broken almost at the same time, leading to the transmission path of the internal force was cut off totally and the inner torsional moment disappeared. Thus, the phenomenon that the steel wires spread out cannot be observed.

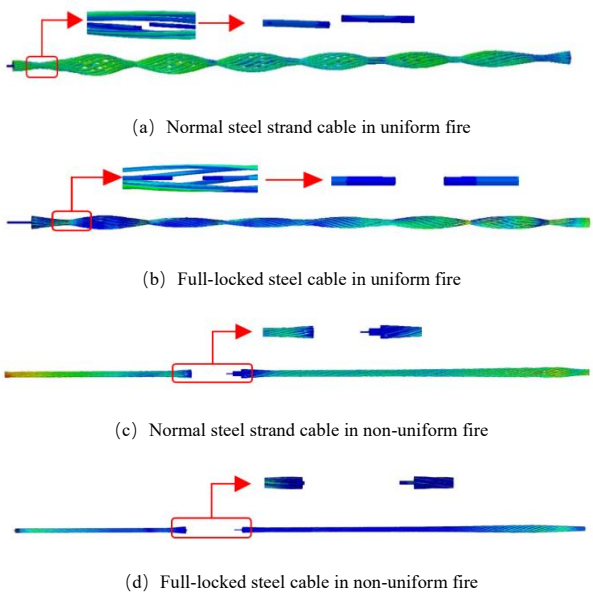

(a) Normal steel strand cable in uniform fire

(b) Full-locked steel cable in uniform fire

(c) Normal steel strand cable in non-uniform fire

(d) Full-locked steel cable in non-uniform fire

Fig. 9 Damage location and mode of steel cable under large-space fire

3.5.2. Axial deformation and fire resistance

As shown in Fig. 10, the axial displacement-time curves of the steel cables under the two fire conditions are acquired. In the uniform fire condition, the fire resistance of the normal steel strand cable was 77.18 min, and that of the full-locked steel cable was 98.98 min. In the non-unform fire condition, the fire resistance of the normal steel strand cable was 80.20 min, and that of the full-locked steel cable was 101.90 min.

The axial deformation of the steel cables was in a growing trend in the heating process, but the deformation rate of which was changing. In the heating period of 20 ~ 40 min, the axial displacement of the steel cable increased rapidly, this is because, in this period, the steel cables are in the necking stage, the first and the second layer of steel wires entered the plastic state, causing the axial deformation rate of the steel cables increases.

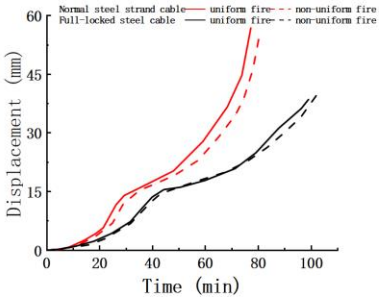

Fig. 10 Axial displacement-time curves of steel cables

3.5.3. Energy analysis

According to the energy conservation, the external work done by the tensile force loaded on the steel cable is mainly converted into the internal strain energy, the internal energy mainly caused by thermal expansion and the friction energy dissipation (energy dissipated by overcoming friction between the steel wires). The relevant data of the overall external work, friction energy dissipation and internal strain energy of the steel cables were directly extracted in the post-processing program of Abaqus. The internal non-strain energy mainly caused by thermal expansion was obtained by subtracting the internal strain energy and friction energy dissipation from the external work of the steel cables.

Fig.11 presents the variation curves of the proportion of the internal strain energy to the external work and the variation curves of the proportion of the internal non-strain energy mainly caused by thermal expansion to the external work during the heating process under different fire conditions.

As shown in Fig.11, thermal expansion primarily caused the deformation development of the steel cables during the early stage of heating; while in the middle and late period of heating, stress deformation mainly caused the deformation development. The reason is that, during the early stage of the heating process, the extent of material strength deterioration is low. With the elevation of temperature, the extent of the deterioration is gradually deepened, so that the axial displacement increases over time. During the middle and late period of heating process, the temperature-elevation rate of the steel cables gradually decreases, leading to the development of thermal expansion deformation slows down.

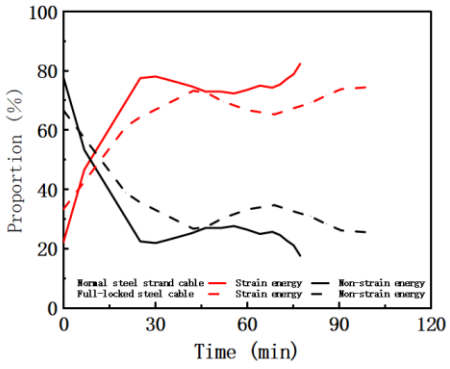

(a) Unform fire condition

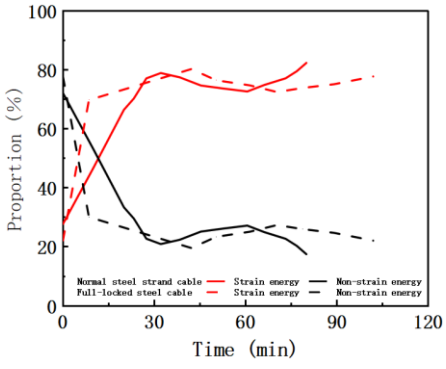

(a) Non-uniform fire condition

Fig. 11 Contribution analysis of axial deformation of steel cables

3.5.4. Internal force development of steel wires

Fig.12 shows the development of the average internal force of the steel wires at the mid-span position under the uniform fire. Fig.13 shows the internal force development of the steel wires at the boundary of the fire position and the non-fire position under the non-uniform fire.

Fig.12 and Fig.13 show that the average internal force of the first two layer of steel wires increased and then declined, while the average internal force of the third layer of steel wires decreased first, then increased and finally destroyed.

It indicated the internal force was redistributed in the steel cables under the fire condition. The reason is that, during the early stage of the heat up time, compared with the first two layer of steel wires, the third layer of steel wires exposed directly to the high-temperature environment has deeper extent of material strength deterioration and thermal expansion deformation, and the tensile stiffness of which is lower due to the larger twist angle. Thus, in this stage, the tensile force loaded on the steel cables is mainly borne by the first two layer of steel wires. When the steel cables enter the necking stage, the first two layer of the steel wires begin to deform plastically, causing the tensile stiffness decreases sharply. And at this moment, the internal force starts to transfer from the first two layer of steel wires to the third layer of steel wires.

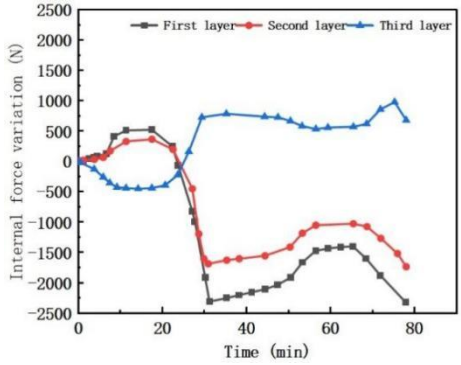

(a) Normal steel strand cable

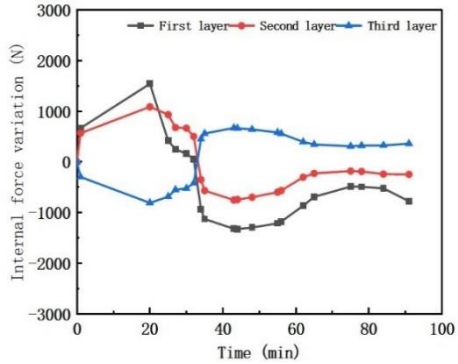

(b) Full-locked steel cable

Fig. 12 Development of average internal force of steel cable in uniform fire

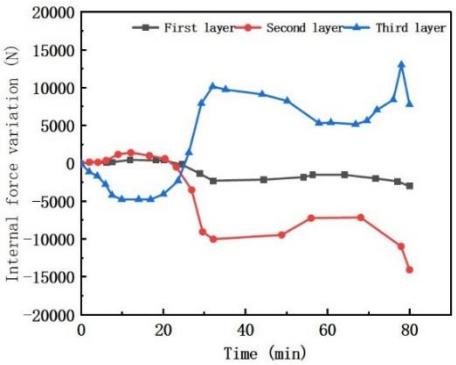

(a) Normal steel strand cable

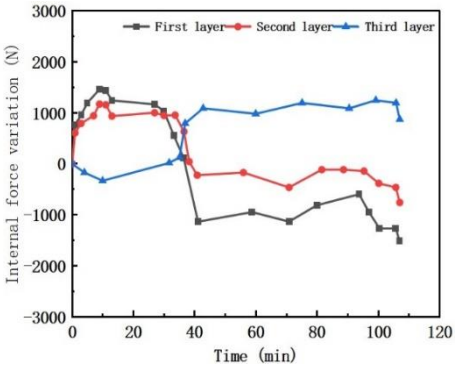

(b) Full-locked steel cable

Fig. 13 Development of average internal force of steel cable in non-uniform fire

3.5.5. Contact stress development

Taking the mid-span section of the steel cables under the uniform fire as the object, where the contact stress during the heat up time was analyzed. Fig.14 shows the arrangement of the contact points of the section.

Fig.15 shows the development of the contact stress over time. Overall, the contact stress of the steel wires declined over time, especially the contact relationships between A33, B33, A21 and B21 were the most sensitive. This is because as the temperature rises, due to the spiral decoupling of the steel wires, the deformation of the transverse section gradually increases, causing the overall contact stress between the steel wires decreases over time.

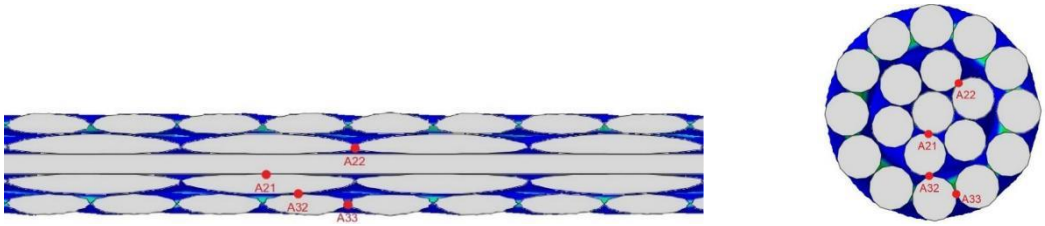

(a) Y-Z section and transverse section of normal steel strand cable

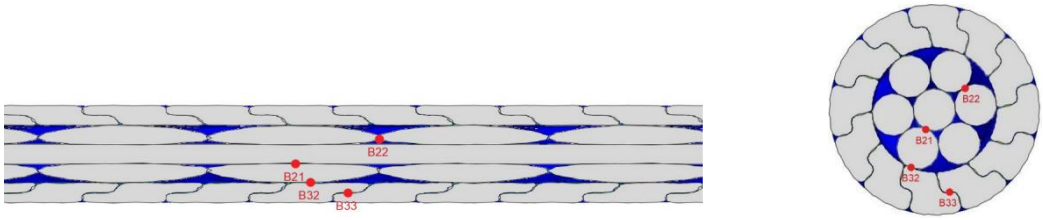

(b) Y-Z section and transverse section of full-locked steel cable

Fig. 14 Arrangement of contact points between steel wires

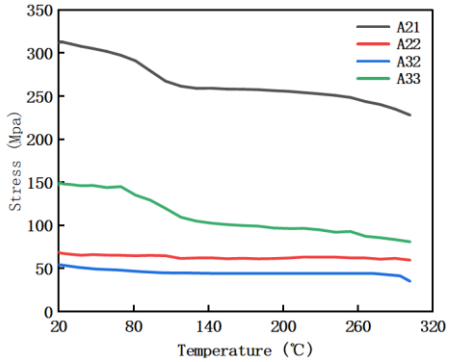

(a) Normal steel strand cable

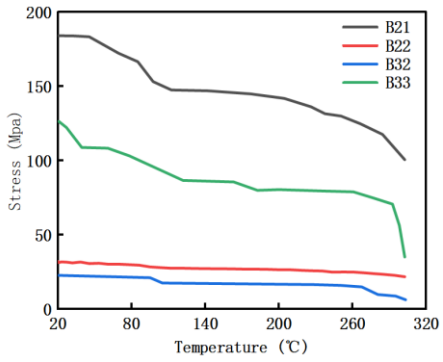

(b) Full-locked steel cable

Fig. 15 Stress-temperature curves of steel cables

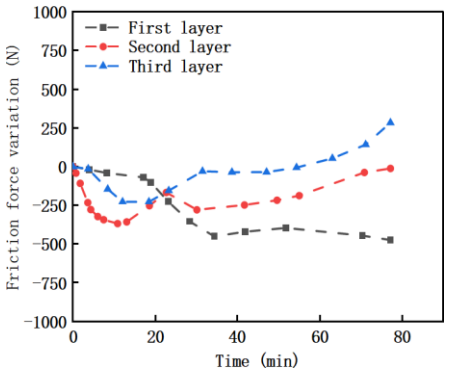

(a) Normal steel strand cable

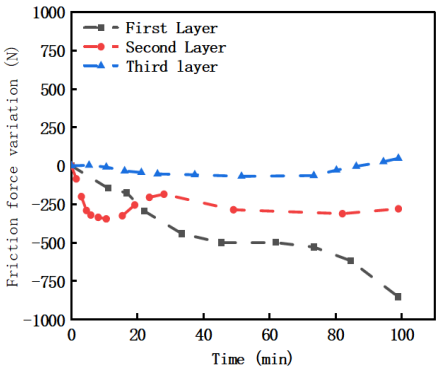

(b) Full-locked steel cable

Fig. 16 Variation of average resultant force of friction of steel cables

Taking the steel cables under the uniform fire as the object , the average resultant force of friction between each layer of steel wire was analyzed. Fig.16 shows the variation of the average resultant force of friction.

Fig.16 shows that the average resultant force of friction of the normal steel strand cable and the full-locked steel cable was much smaller than the contact stress of the steel cables, which indicated that the friction contributed little to the force transmission inside the steel cable. With the increase of time, the average resultant force of friction of the first two layer of steel wires presented a decreasing trend in general. Combined with the phenomenon that the contact stress decreased with the elevated temperature, it indicated that the contact relationship of the steel wires had been weakened in general. In addition, as the internal force of the first two layer of steel wires was transferred to the third layer of steel wires over time, the average resultant force of friction of the third layer of steel wire declined with time.

4. Parametric analysis of steel cable in large-space fire

In this section, the numerical investigation of 41 normal steel cables was carried out. The parametric analysis of the fire-resistant capacity and the deformation development of the normal steel cable was performed.

4.1. Effect of temperature-field model for large-space fire

The parametric investigation on the fire-resistant capacity of the steel cable was conducted under the large-space building fire condition, including the parameters of floor area, position height of steel cable, fire grow type and heat release rate, and the numerical examples for which are shown in Table 1. In Table 1, the non-uniform level η denotes the ratio of the span of the unburned part to the total span of the steel cables. When the non-uniform level η is 0, it indicates the steel cable is uniformly subject to fire along the whole span. In addition, in reference to the literature [6], the parameter of load ratio in Table 1 denotes the ratio of the horizontal tension to the ultimate break force of the steel cable after the design load is applied at room temperature. In this section, the ultimate break force of the numerical examples is 1253.36 KN, and the other geometric parameters not given in Table 1 are consistent with the FE model of the normal steel strand cable stated in section 2.1.

Table 1
Numerical examples for parametric analysis of temperature-field model

Specimen	Floor area A_{sp}（mm²）	Position height H（m）	Factor of fire growth type γ	Fire release rate Q（MW）	Non-uniform level η	Load ratio R	Span L（m）
RF-0	500	6	0.004	25	0	0.3	15
Area-1	1000	6	0.004	25	0	0.3	15
Area-2	3000	6	0.004	25	0	0.3	15
Area-3	6000	6	0.004	25	0	0.3	15
Height-1	500	11	0.004	25	0	0.3	15
Height-2	500	16	0.004	25	0	0.3	15
Height-3	500	21	0.004	25	0	0.3	15
Height-4	500	26	0.004	25	0	0.3	15
Growth-1	500	6	0.001	25	0	0.3	15
Growth-2	500	6	0.002	25	0	0.3	15
Growth-3	500	6	0.003	25	0	0.3	15
Power-1	500	6	0.003	12	0	0.3	15
Power-2	500	6	0.003	14	0	0.3	15
Power-3	500	6	0.003	16	0	0.3	15
Power-4	500	6	0.003	19	0	0.3	15
Power-5	500	6	0.003	22	0	0.3	15

4.1.1. Floor area

As shown in Fig.17, in the condition of remaining other parameters unchanged, when the building area rose from 500 m² to 6000 m², the fire resistance rose from 141 min to 455 min. The lag phenomenon of the axial deformation development of the steel cable was deepened when the floor area increased, and the fire resistance increased in nonlinear tendency. This is because as the floor area increases, the ambient temperature of the large-space building decreases in nonlinear tendency, causing the lagging development of the material strength deterioration, the thermal creep and the axial deformation caused by thermal expansion.

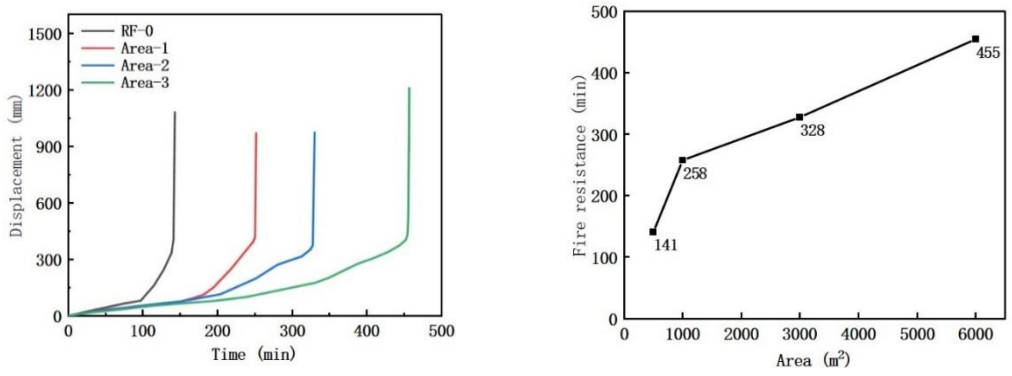

(a) Effect on axial deformation (b) Effect on fire resistance

Fig. 17 Parametric analysis of floor area on steel cable

4.1.2. Position height

As shown in Fig.18, in the condition of remaining other parameters unchanged, when the position height increased from 6m to 26m, the fire resistance rose from 141 min to 341 min. The lagging phenomenon of axial deformation development of the steel cable was deepened when the position height of the steel cables increased, leading to the higher fire resistance.

This is because according to the temperature-field model for large-space fire, the greater position height leads to the lower elevated temperature of the steel cable, which causes the lagging development of the material strength deterioration, the thermal creep and the axial deformation caused by thermal expansion under the same heat up time.

4.1.3. Fire growth type

As shown in Fig.19, in the condition of remaining other parameters unchanged, the fire resistance declined from 187 min to 141 min, as the fire growth type rose from 0.001 to 0.004. During the early stage of the heat up process, the fire growth type had little difference in the deformation development, but the difference in the deformation development gradually became larger over time. As the fire growth rate increased, the fire resistance of the steel cable presented a nonlinear downward trend. Compared to the other parameters, the increase of the fire growth type had little influence on the downward trend of the fire resistance.

4.1.4. Heat release rate

As shown in Fig.20, in the condition of remaining other parameters unchanged, when the heat release rate rose from 14 MW to 25 MW, the fire resistance decreased from 434 min to 141 min. As the heat release rate of the steel cables increasing, the fire resistance of the steel cables reduced over time, and the difference in the deformation development was greater. The heat release rate of the fire had the significant effect on the fire resistance.

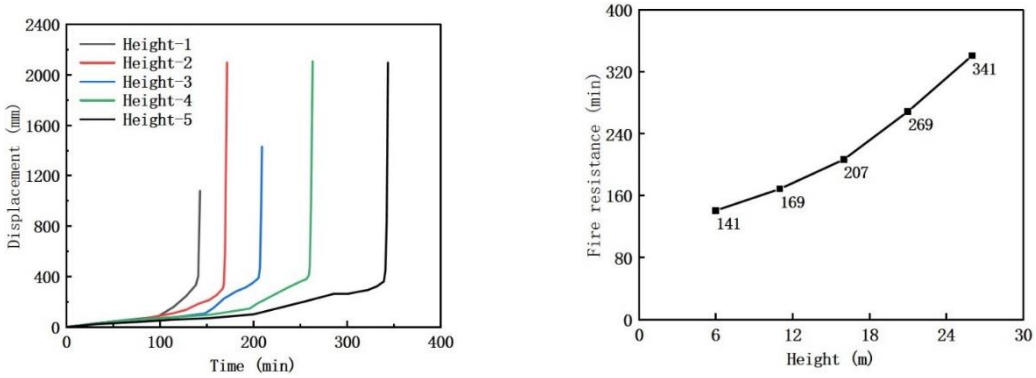

(a) Effect on axial deformation (b) Effect on fire resistance

Fig. 18 Parametric analysis of position height of steel cable

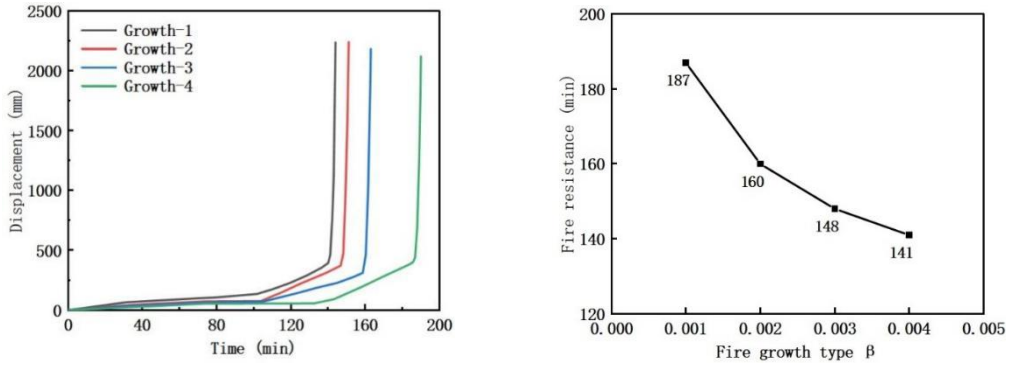

(a) Effect on axial deformation (b) Effect on fire resistance

Fig. 19 Parametric analysis of fire growth

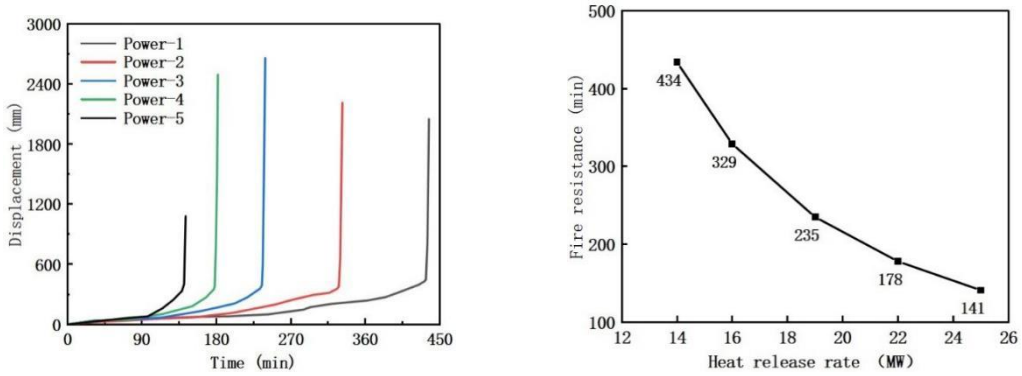

(a) Effect on axial deformation (b) Effect on fire resistance

Fig. 20 Parametric analysis of heat release rate of fire

4.2. Non-uniform level of fire and fire source location

The parameter of non-uniform level of fire is set ranging from 0~0.8, and the non-uniform fire is located at the mid-span and the end of steel cable. As the non-uniform fire is located at the mid-span, the non-uniform fire extends from the middle to both ends of the steel cable; as the non-uniform fire is located at the end of the steel cable, the non-uniform fire extends from the one end to the other end. In addition, for the other parameters, the floor area is 500 m^2; the position height is 6 m; the factor of fire growth type is 0.004; the load ratio is 0.3; the fire release rate is 25 MW; the span is 15 m.

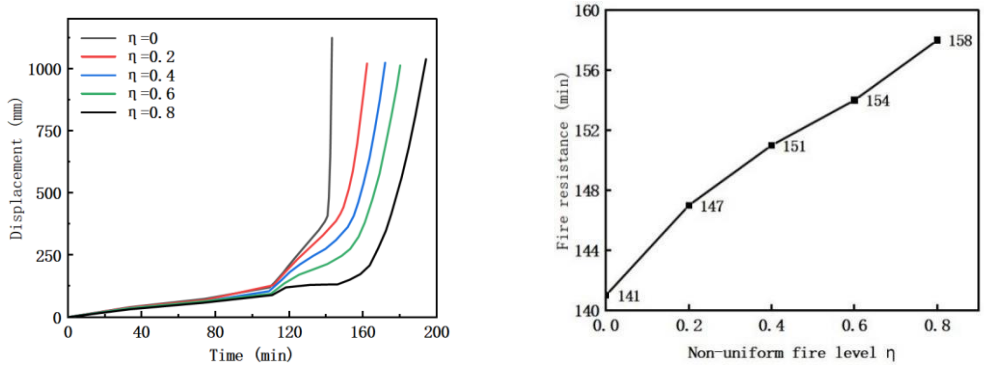

(a) Effect on axial deformation (b) Effect on fire resistance

Fig. 21 Parametric analysis of non-uniform level of fire at mid-span of steel cable

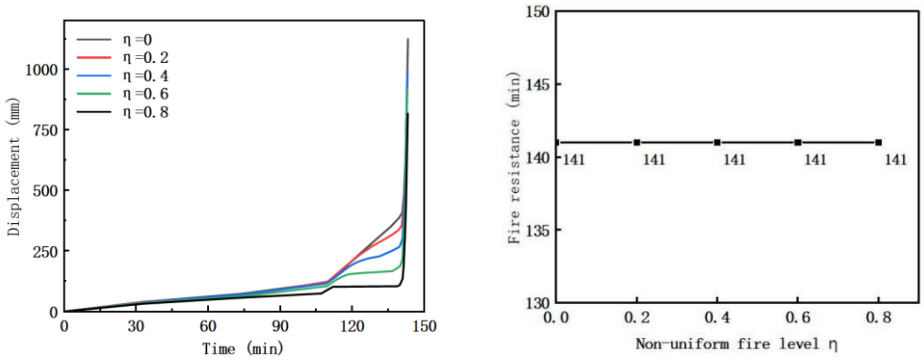

(a) Effect on axial deformation (b) Effect on fire resistance

Fig. 22 Parametric analysis of non-uniform level of fire at end of steel cable

Fig.21 and Fig.22 show the effect of non-uniform level of fire and fire source location on the deformation and the fire resistance.

Fig.21 shows that, when the fire was set at the mid-span, with the increase of the non-uniform level, the deformation of the steel cable was smaller and the fire resistance was higher. The reason is that the increasing continuous area of the steel cable causes more heat absorption under the non-uniform fire condition, which makes the accumulated axial deformation due to thermal expansion and thermal creep larger. Thus, the strain of the steel wire reaches the rupture strain early, and the fire resistance decreases.

As shown in Fig. 22, when the fire source was set at the end of the steel cable, with the increase of the non-uniform level, the deformation of the steel cable was smaller, but the fire resistance did not change. The reason is the damage of the specimens with fire at the end is induced by the fact that the first layer of steel wires at the loading end reaches the rupture strain first, and breaks at the necking part near the end, which is different from the failure mode when the steel cable is subject to the fire source located under the mid-span. It indicates the failure pattern of the steel cable is mainly related to the location of fire source.

4.3. Load ratio

The parameter of load factor is set ranging from 0.2~0.7. The non-uniform level of fire is set as 0. For the other parameters, the floor area is 500 m^2; the position height is 6 m; the factor of fire growth type is 0.004; the fire release rate is 25 MW; the span is 15 m.

As shown in Fig.23, in the condition of remaining other parameters unchanged, the fire resistance decreased from 158 min to 87 min, as the load ratio rose from 0.2 to 0.7. As the load ratio increasing, the deformation was larger and the fire resistance declined in nonlinear tendency, indicating that the parameter of load ratio greatly affects the fire behavior of the steel cables.

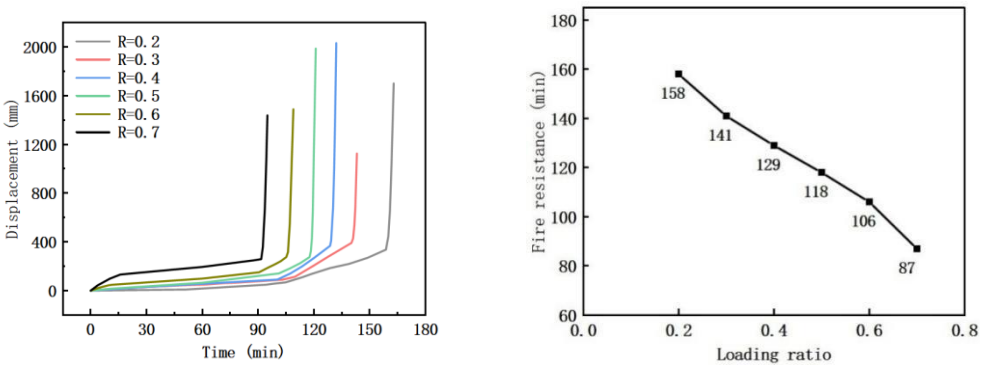

(a) Effect on axial deformation (b) Effect on fire resistance

Fig. 23 Parametric analysis of load ratio

4.4. Span

The parameter of fire source location is set under the mid-span and the end of steel cable. The non-uniform fire level is set ranging from 0~0.8. The span is set ranging from 15 ~35 m. In addition, the floor area is 500 m^2; the position height is 6 m; the factor of fire growth type is 0.004; the fire release rate is 25 MW ;the load ratio is 0.3. Fig. 24 shows the parametric analysis result.

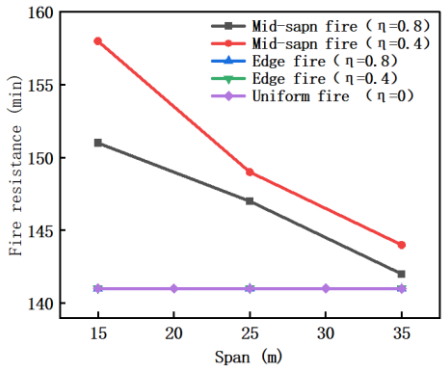

Fig. 24 Parametric analysis of span under different fire conditions

According to Fig.24, the fire resistance of the specimens subject to the edge fire is the same as that of the specimens subject to uniform fire, which is 141 min. When the end part of the steel cables was directly exposed to fire, the specimen was damaged earlier than when the mid-span position was exposed to fire. This phenomenon is consistent with the conclusion pointed out in the literature [6], in which the effect of the non-uniform level of fire on the fire resistance of steel cable was studied. When the end part of the steel cable subject to fire, the fire resistance is independent of the parameter of span and non-uniform level of fire. The uniform fire condition of the steel cable can be taken as the unfavorable working condition in the fire safety design to ensure the reliability of steel cable.

Moreover, it can be found that when the mid-span of the steel cable was subject to fire resource, the fire resistance decreased in nonlinear tendency with the increase of span. And the fire resistance increased as the non-uniform level of fire increased, but with the increase of the span, the influence of the non-uniform level of fire on the fire resistance was weakened.

5. Conclusion

This paper numerically analyzes the fire behavior of the normal steel strand cable and the full-locked steel cable under the large-space building localized fire. The following conclusions for providing fire safety design guidance of steel cable can be drawn:

(1) In the uniform fire condition, the peak temperature difference between the normal steel strand cable and the full-locked steel cable is 138.80 °C, while in the non-uniform fire condition, the maximum temperature difference is 122.05°C. It indicates that the outer surface geometric curvature of the full-locked steel cable is smaller than the outer surface geometric curvature of the normal steel strand cable, which causes that the full-locked steel cable needs to absorb more heat. Therefore, the overall temperature of the normal steel strand cable is higher than that of the full-locked steel cable.

(2) In the fire safety design, it is suggested that the average temperature can be used to simplify the temperature field of the steel cable when calculating the transverse temperature of section, due to the small temperature gradient amplitude of the steel cables(the transverse temperature gradient of normal steel strand cable is 22 °C, and that of the full-locked cable is 17 °C). However, the longitudinal temperature gradient amplitude of the two types of steel cables is large (the longitudinal temperature gradient of normal steel strand cable is 81 °C, and that of the full-locked steel cable is 79 °C), which cannot be ignored in fire safety design.

(3) In the condition of remaining other parameters unchanged, when the floor area increases from 500 m^2 to 6000 m^2, the fire resistance of the steel cable rises from 141 min to 455 min ; when the position height increases from 6m to 26m, the fire resistance rises from 141 min to 341 min; when the fire growth type rises from 0.001 to 0.004, the fire resistance decreases from 187 min to 141 min; when the heat release rate rises from 14 MW to 25 MW, the fire resistance decreases from 434 min to 141 min; as the load ratio increases from 0.2 to 0.7, the fire resistance decreases from 158 min to 87 min. The effect extent of the parameter in the model on the steel cable is as follows: heat release rate, position height of steel cable, floor area, fire growth type. In addition, the parameter of load ratio greatly affects the fire resistance.

(4) The influence of non-uniform level of fire and span on the fire resistance of the steel cable is related to the fire location. When the fire location is at the end of the steel cable, the non-uniform level of fire and the span have no effect on the fire resistance. When the fire location is only at the mid-span of the steel cable, the non-uniform level of the mid-span fire increases from 0 to 0.8, the fire resistance of the steel cable increases from 141 min to 158 min. In the condition of remaining other parameters unchanged, the fire resistance decreases with the increasing span, the span factor greatly affects on the fire resistance.

(5) The influence of span on the fire resistance under different fire conditions is analyzed, including the fire conditions of non-uniform fire at the mid-span of steel cable, non-uniform fire at the span end and uniform fire. It is found that the uniform fire condition can be regarded as the most unfavorable fire condition of the steel cable in the fire safety design.

Notations

λ_s-Thermal conductivity of steel
λ_i- Equivalent thermal conductivity of non-swelling fire protection coating
R_i- Equivalent thermal resistance of intumescent fire protection coating
H- Position height
T_g^{max}-Maximum air temperature
Q- Heat release rate
A_{sp}- Floor area
A_q- Fire area
γ- Factor of fire growth type
K_{sm}- Factor for regression ratio of maximum air temperature
β- Shape factor dependent on the floor area and space height
C_s- Specific heat capacity
T_{st}- Temperature of steel material
σ- Stress of steel wires
ε- Strain of steel wires
E- Elastic modulus of steel wires
$\varepsilon_{pp,\theta}$- Proportional limit strain at elevated temperature
$\varepsilon_{pt,\theta}$- Limit strain for yield strength at elevated temperature
$\varepsilon_{pu,\theta}$- Rupture strain at elevated temperature
ε_{th} – Thermal expansion strain
α_T- Thermal expansion coefficient
T- Temperature of steel wires
ε_{cr}- Creep strain at elevated temperature

Acknowledgments

The investigation was supported by the General Program of National Natural Science Foundation of China (52278136), and the General Program of National Natural Science Foundation of China (52378118).

Reference

[1] J. Lu, S.D. Xue, X. Y. Li, Experiment study on the influences of length errors of cables and struts on spatial cable-truss structure without inner ring cables [J]. Adv. Steel Constr. 19(2) (2023) 112-120.
[2] J. Lu, S.D. Xue, X.Y. Li, Q. Liu, Study on static and dynamic experiment of spatial cable-truss structure without inner ring cables based on grid-jumped layout of struts [J]. Adv. Steel Constr. 18(4) (2022) 783-792.
[3] J. Lu, S.D. Xue, X. Y. Li, M. Dezhkam, Segmented assembly construction forming method without brackets of spatial cable-truss structure without inner ring cables [J]. Adv. Steel Constr. 18(3) (2022) 687-698.
[4] J. Lu, X. Y. Li, S.D. Xue, R.J Liu, M. Dezhkam, Study on force mechanism of cable-truss frame and jumped layout of annular crossed cable-truss structure [J]. Adv. Steel Constr. 17(3) (2022) 243-252.
[5] A.L. Zhang, W.J. Rao, W.L. Cui, Stability analysis of pre-stress loss on suspend-dome structure under fire hazard [J]. J. Beijing Uni. Technol. 8 (36) (2010) 1044-1051 (in Chinese). doi:10.11936/bjutxb2010081044.
[6] Y. Du, J.Y. Richard Liew, H. Zhang, G.Q. Li, Pre-tensioned steel cables exposed to localized fires [J]. Adv. Steel Constr. 14(2) (2018) 206-226. Doi: 10.18057/IJASC.2018.14.2.5.
[7] M.F. Day, E.A. Jenkinson, A.I. Smith, Effect of elevated temperatures on high-tensile-steel wires for prestressed concrete [J]. Proc. Inst. civ. Eng. 16 (5) (1960) 55-70. https://doi.org/10.1680/iicep.1960.11781.
[8] J. Gales, L.A. Bisby, T. Strafford, New parameters to describe high-temperature deformation of prestressing steel determined using digital image [J].Correlation, Struct. Eng. Int. 22 (4) (2012) 476–486. https://doi.org/10.2749/ 101686612X13363929517730.
[9] X.M. Hou, W.Z. Zheng, V. Kodur, H.Y. Sun. Effect of temperature on mechanical properties of prestressing bars [J].Constr. Build. Mater. 61 (6) (2014) 24-32. https://doi.org/10.1016/j.conbuildmat.2014.03.001.
[10] G.J. Sun, Z.H. Li, J.Z. Wu, J.Y. Ren, Investigation of steel wire mechanical behavior and collaborative mechanism under high temperature [J]. J. Constr. Steel Res.188 (2022) 107039. https://doi.org/10.1016/j.jcsr.2021.107039.
[11] Z. Zong, D. Jiang, J. Zhang, Study of the mechanical performance of grade 1860 steel wires at elevated temperatures [J]. Mater. Res. Innov. 19 (suppl.5) (2015), S5.1175-S5.1181. http://dx.doi.org/10.1179/1432891714Z.0000000001273.
[12] P. Kotsovinos, A. Atalioti, N. McSwiney, F. Lugaresi, G. Rein, A.J. Sadowski, Analysis of the thermo-mechanical response of structural cables subject to fire [J]. Fire Technol. (2019) 1–29, https://doi.org/10.1007/s10694-019-0.
[13] Y. Du, J.Z. Peng, J.Y. Richard Liew, G.Q. Li, Mechanical properties of high tensile steel cables at elevated temperatures [J]. Constr. Build. Mater. 182 (2018) 52-65. https://doi.org/10.1016/j.conbuildmat.2018.06.012.
[14] Y. Du, H.H. Qi, J. Jiang, J.Y. Richard Liew, G.Q. Li, Mechanical properties of 1670 MPa parallel wire strands at elevated temperatures [J]. Constr. Build. Mater. 263 (2020) 120582. https://doi.org/10.1016/j.conbuildmat.2020.120582.
[15] Y. Du, J.Y. Richard Liew, J. Jiang, G.Q. Li, Improved time-hardening creep model for investigation on behavior of pre-tensioned steel strands subject to localized fire [J]. Fire Saf. J. 116 (2020) 103191. https://doi.org/10.1016/j.firesaf.2020.103191.
[16] G.J. Sun, J. Yuan, S.D. Xue, Y. Yang, M. Mensinger, Experimental investigation of the mechanical properties of zinc-5% aluminum-mixed mischmetal alloy-coated steel strand cables [J]. Constr. Build. Mater. 233 (2020) 117310.
[17] G.J. Sun, X.H. Li, J.Z. Wu, R.H. Chen, G.N. Chen, Deformation of stainless steel cables at elevated temperature [J]. Eng. Struct. 211 (2020) 110498. https://doi.org/10.1016/j.engstruct.2020.110498.
[18] G.J. Sun, S. Xiao, X.S. Qu, Thermal–mechanical deformation of Galfan-coated steel strands at elevated temperatures [J]. J. Constr. Steel Res. 180 (2021) 106574. https://doi.org/10.1016/j.jcsr.2021.106574.
[19] E.F. Du, X.B. Hu, Z. Zhou, Q. Li, X. Lyu, Y.Q. Tang, Experimental investigation on mechanical properites of Grade 1670 steel wires under and after elevated temperature [J]. Adv. Steel Constr. 19(1) (2023) 9-16.
[20] Y. Du, Y.K. Sun, J. Jiang, G.Q. Li, Effect of cavity radiation on transient temperature distribution in steel cables under ISO834 fire [J]. Fire Saf. J. 104 (2019) 79-89. https://doi.org/10.1016/j.firesaf.2019.01.002.
[21] V. Fontanari, M. Benedetti, B.D. Monelli, F. Degasperi, Fire behavior of steel wire ropes: Experimental investigation and numerical analysis [J]. Eng. Struct. 84 (2015) 340-349. http://dx.doi.org/10.1016/j.engstruct.2014.12.004.
[22] V. Fontanari, M. Benedetti, B.D. Monelli, Elasto-plastic behavior of a Warrington-Seale rope: Experimental analysis and finite element modeling [J]. Eng. Struct. 82 (2015) 113-120. http://dx.doi.org/10.1016/j.engstruct.2014.10.032.
[23] GB 51249-2017, Code Fires Safety Steel Building Structures [S]. China Planning Press, Beijing, 2017.
[24] G.Q. Li, Y. Du, A new temperature-time curve for fire-resistance analysis of structures [J]. Fire Saf. J. 54 (2012) 113-120. http://dx.doi.org/10.1016/j.firesaf.2012.07.004.
[25] EN 1991-1-2, General actions-actions on structures exposed to fire, European Committee for Standardization [S]. Brussels, 2002.
[26] J.R. Welty, G.L. Rorrer, C.E. Wicks, C.E. Wicks. Fundamentals of momentum, heat, and mass transfer, fifth ed. [M]. Wiley, State of New Jersey, 2008.
[27] R. M. Lawson , G. M. Newman, PUB 080 Fire Resistant Design Of Steel Structures: A Handbook To Bs 5950: Part 8 [S]. The Steel Construction Institute, Ascot,1990.
[28] H. Zhou, Y. DU, G.Q. Li, J.Y. Richard Liew, X.C. Wang, Experimental study on thermal expansion and creep properties of pre-stressed steel strands at elevated temperature [J]. Eng. Mech. 35(06) (2018) 123-131. (in Chinese). Doi: 10.6052/j.issn.1000-4750.2017.02.0155
[29] G.Y. Wang, Y.D. Meng, R.J. Liu, Liu Werihua. An experimental research on the fire resistance of steel cable structures and its finite element analysis [J]. J. Build. Struct. :1-8[2022-09-16]. (in Chinese). DOI:10.14006/j.jzjgxb.2021.0563.
[30] L.L. Wang, G.Q. Li, Y.Y. Xu, W.H. Wang, Insulating properties of intumescent coating for steel element under different fire conditions [J]. J. Build. Mater. 19 (02) (2016), 267-273+279. (in Chinese). doi:10.3969/j. issn.1007-9629.2016.02.010.
[31] G.Q. Li, P.J. Wang . Advanced Analysis and Design for Fire Safety of Steel Structures [M]. Advanced Topics in Science and Technology in China, Zhejiang, 2013.